

BRIGT

Erasmus+ strategic partnership for Higher Education

BOOSTING THE SCIENTIFIC EXCELLENCE AND INNOVATION
CAPACITY OF 3D PRINTING METHODS IN PANDEMIC PERIOD

O4 - BRIGT CAE e-learning webinar

Project Title	Boosting the scientific excellence and innovation capacity of 3D printing methods in pandemic period 2020-1-RO01-KA226-HE-095517
Output	O4 - BRIGT e-learning webinars on the use of 3D printing technologies in development, testing and producing of medical parts in pandemic period – CAE e-learning webinar description
Date of Delivery	30 November 2022
Authors	Dan-Sorin Comşa, Răzvan Păcurar
Version	FINAL VERSION

This project has been funded with support from the European Commission. This publication [communication] reflects the views only of the author, and the Commission cannot be held responsible for any use which may be made of the information contained therein.

Content

1. Introduction.....	3
2. Description of the webinar.....	3
2.1. Structure of the webinar	3
2.2. Steps of the webinar described in detail and methods used for teaching	4
2.2.1. Finite element analysis of a wrist hand orthosis (1st case study).....	4
2.2.2. Finite element analysis of a tongue casting mould (2nd case study)	8
2.2.3. Finite element analysis of a face shield base (3rd case study)	14
2.3. Importance of the webinar and of the presented results.....	19
3. Conclusions.....	19

This project has been funded with support from the European Commission. This publication [communication] reflects the views only of the author, and the Commission cannot be held responsible for any use which may be made of the information contained therein.

1. Introduction

Engineering calculations are essential components of the design process. Any equipment must be designed in such a way that its functionality is ensured while satisfying different requirements related to cost, overall dimensions, manufacturing procedures, reliability, etc. Such requirements often lead to the imposition of some constraints whose fulfilment should be assessed by engineering calculations (for example, not exceeding a maximum stress, strain, or deflection level, guaranteeing the fatigue strength, etc.). Engineering calculations provide the information from which the designer can deduce how close the equipment is to the limit states that could compromise its functionality.

The CAE webinar has focused on providing the students with the basic knowledge of applying the finite element method in the design of medical devices. Three case studies have been considered. They have consisted in the computer simulation of different tests meant to evaluate the strength characteristics of a wrist hand orthosis, a tongue casting mould, and a face shield base. The finite element analysis module SOLIDWORKS Simulation (component of the SOLIDWORKS computer-aided design software package) has been used to perform the tests [<https://www.solidworks.com> , <https://www.solidworks.com/product/solidworks-simulation>]. The webinar is available on the BRIGHT project website by accessing the following link: <https://bright-project.eu/?p=342>

Webinar can be accessed directly also from YouTube, by accessing the following link: <https://www.youtube.com/watch?v=HvELM896GPc>

2. Description of the webinar

2.1. Structure of the webinar

The webinar has been divided into three parts, each of them being devoted to the presentation of a case study in the following steps:

- Emphasizing the objectives of the case study
- Describing the medical device to be analysed
- Describing the test to be simulated with the aim of evaluating the strength characteristics of the medical device
- Detailing the preparation of the finite element model of the test with SOLIDWORKS Simulation
- Analysing the numerical results provided by SOLIDWORKS Simulation

This project has been funded with support from the European Commission. This publication [communication] reflects the views only of the authors, and the Commission cannot be held responsible for any use which may be made of the information contained therein.

- Formulating some conclusions.

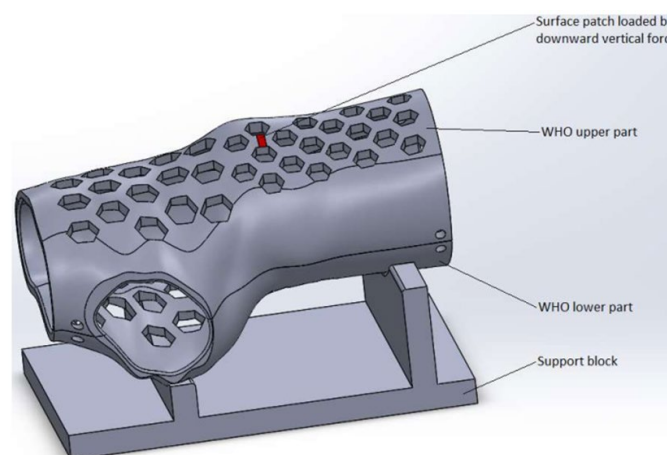
The most significant aspects of the finite element analysis of medical devices have been approached during the presentation of the case studies (see §2.2 for details):

- Defining material properties
- Specifying contact interactions
- Enforcing various types of boundary conditions (kinematic constraints and external loads)
- Controlling the size of finite elements
- Generating the finite element mesh
- Postprocessing the numerical results.

2.2. Steps of the webinar described in detail and methods used for teaching

2.2.1. Finite element analysis of a wrist hand orthosis (1st case study)

The first case study has focused on evaluating the strength characteristics of a wrist hand orthosis by simulating a three-point bending test [<https://doi.org/10.3390/ma13194379>]. The principle of the test is shown in Figure 1. As one may notice, the lower and upper parts of the orthosis are assembled and placed on a support block. The upper part of the orthosis is then loaded by a downward vertical force acting on the red surface patch. This load gradually increases from 0 (zero) to 125 N. The contact between the lower part of the orthosis and the support block takes place along perfectly matching surfaces.



This project has been funded with support from the European Commission. This publication [communication] reflects the views only of the authors, and the Commission cannot be held responsible for any use which may be made of the information contained therein.

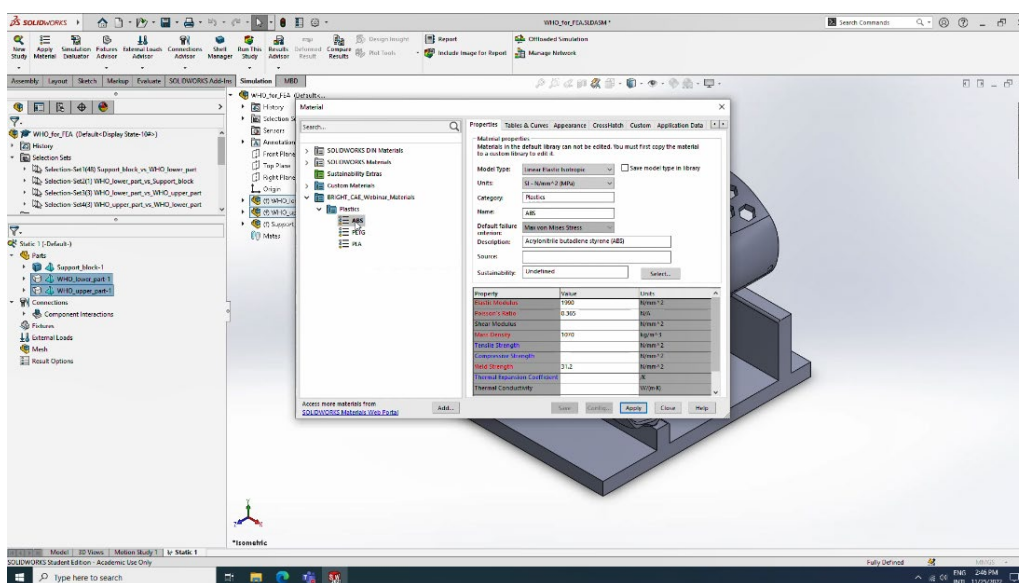
Figure 1. Principle of the three-point bending test simulated for evaluating the strength characteristics of the wrist hand orthosis (frame extracted from the recording of the CAE webinar)

The following assumptions have been made when preparing the finite element model of the three-point bending test:

- The lower and upper parts of the orthosis are made from ABS exhibiting an isotropic linear elastic behaviour. Table 1 lists the physical and mechanical properties of ABS that are relevant for the finite element model of the three-point bending test. These parameters have been stored in the custom library BRIGHT_CAE_Webinar_Materials.sldmat (see Figure 2) provided to the students together with the 3D model shown in Figure 1.
- The support block is a perfectly rigid body.
- The lower and upper parts of the orthosis are bonded together along their contact surfaces.
- The lower part of the orthosis is allowed to slide along its contact surfaces with the support block. The frictional component of this contact interaction is neglected.

Table 1. Physical and mechanical properties of ABS [https://doi.org/10.1007/978-3-319-41600-7_11]

Mass density ρ [kg/m ³]	Elastic modulus E [MPa]	Poisson's ratio ν [-]	Yield strength Y [MPa]
1070	1990	0.365	31.2



This project has been funded with support from the European Commission. This publication [communication] reflects the views only of the authors, and the Commission cannot be held responsible for any use which may be made of the information contained therein.

Figure 2. Associating the ABS material to the lower and upper parts of the orthosis by accessing the BRIGHT_CAE_Webinar_Materials.sldmat library (frame extracted from the recording of the CAE webinar that is available on the BRIGHT Virtual laboratory platform on TUCN room)

The following steps have been performed for preparing the finite element model of the three-point bending test:

- a) Defining the pressure block (Fig. 1) as a perfectly rigid body
- b) Associating the ABS material to the lower and upper parts of the orthosis (Fig. 1) by accessing the BRIGHT_CAE_Webinar_Materials.sldmat library (Fig. 2)
- c) Specifying the contact interaction between the support block and the lower part of the orthosis (Fig. 1): frictionless sliding contact (Fig. 3)
- d) Specifying the contact interaction between the lower and upper parts of the orthosis (Fig. 1): bonded contact (Fig. 3)
- e) Enforcing a full locking kinematic constraint on the bottom face of the support block (Fig. 3)
- f) Defining a downward vertical unit force applied to the upper part of the orthosis (Fig. 3)
Note: The actual values of this force have been specified later as load cases (step (h)).
- g) Controlling the local and global dimensions of finite elements and generating the mesh (Fig. 3)
- h) Specifying the actual values of the downward vertical force applied to the upper part of the orthosis (Fig. 4): 25 N (load case 1), 50 N (load case 2), 75 N (load case 3), 100 N (load case 4), and 125 N (load case 5).

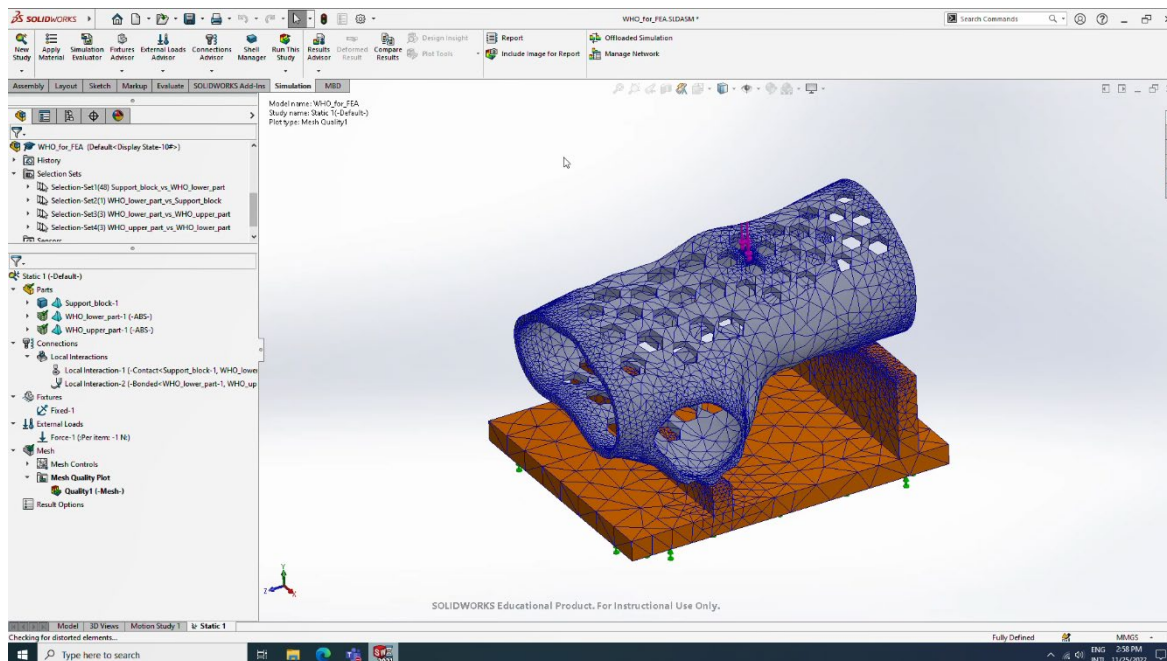


Fig. 3. Finite element model of the three-point bending test simulated for evaluating the strength characteristics of the wrist hand orthosis (frame extracted from the recording of the CAE webinar)

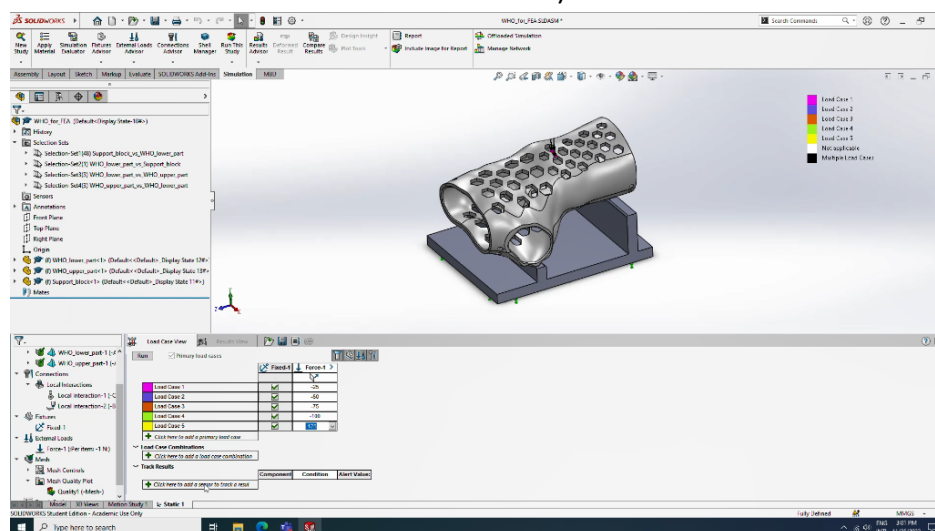


Fig. 4. Specifying the actual values of the downward vertical force applied to the upper part of the orthosis (five load cases): 25 N, 50 N, 75 N, 100 N, and 125 N (frame extracted from the recording of the CAE webinar)

This project has been funded with support from the European Commission. This publication [communication] reflects the views only of the authors, and the Commission cannot be held responsible for any use which may be made of the information contained therein.

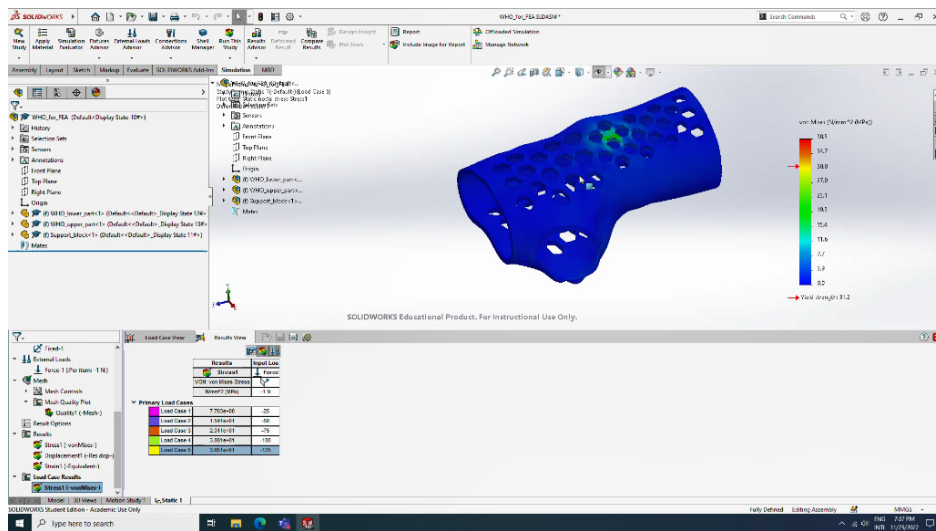


Fig. 5. Colour map showing the distribution of the von Mises equivalent stress in the lower and upper parts of the orthosis for the fifth load case – testing force of 125 N (frame extracted from the recording of the CAE webinar)

Figure 5 shows the most significant result provided by the finite element analysis module SOLIDWORKS Simulation: distribution of the von Mises equivalent stress in the lower and upper parts of the orthosis for the fifth load case (testing force of 125 N). Similar distributions associated to other load cases have also been analysed.

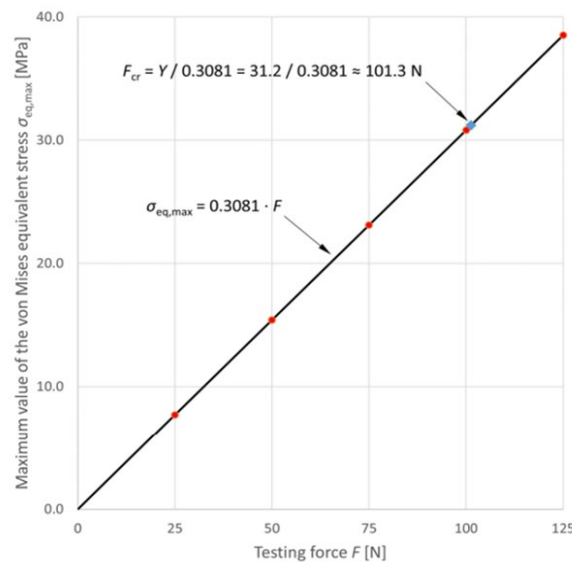


Fig. 6. Maximum values of the von Mises equivalent stress associated to different testing forces: red dots – numerical results; black path – linear regression; blue diamond – testing

This project has been funded with support from the European Commission. This publication [communication] reflects the views only of the authors, and the Commission cannot be held responsible for any use which may be made of the information contained therein.

force at which the maximum value of the equivalent stress equals the yield strength of the ABS material (frame extracted from the recording of the CAE webinar)

The maximum values of the von Mises equivalent stress $\sigma_{eq,max}$ associated to different load cases have been displayed on a diagram showing their dependence on the testing force F (Fig. 6). The following conclusions have been formulated after examining the diagram:

- a) The mechanical response of the orthosis is well approximated by means of the linear regression $\sigma_{eq,max} = 0.3081 \cdot F$ (see the black path displayed on the diagram).
- b) This regression can be used to determine the testing force at which the maximum value of the equivalent stress equals the yield strength of the ABS material: 101.3 N (see the blue diamond displayed on the diagram).

2.2.2. Finite element analysis of a tongue casting mould (2nd case study)

The second case study has focused on evaluating the strength characteristics of a tongue casting mould (Fig. 7) by simulating a pressurization test. The principle of the test is shown in Figure 8. As one may notice, the inner surfaces of the mould parts are loaded by pressure after being clamped between two rigid plates in their assembled configuration. The inner pressure gradually increases from 0 (zero) to 8 MPa.

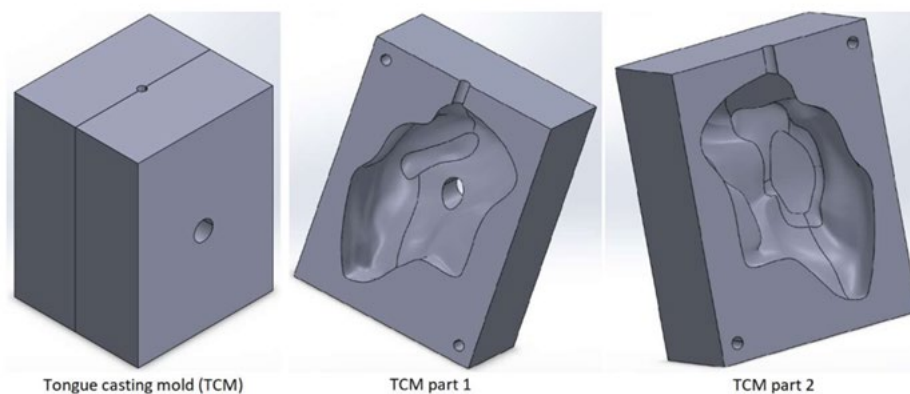


Fig. 7. Three-dimensional model of the tongue casting mould (frame extracted from the recording of the CAE webinar)

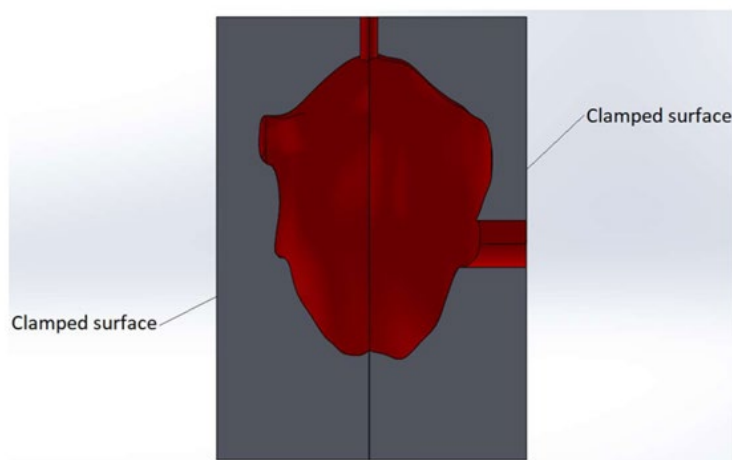


Fig. 8. Principle of the pressurization test simulated for evaluating the strength characteristics of the tongue casting mould: inner pressure acting on the red surfaces (frame extracted from the recording of the CAE webinar)

The following assumptions have been made when preparing the finite element model of the pressurization test:

- a) Both mould parts are made from PLA exhibiting an isotropic linear elastic behaviour. Table 2 lists physical and mechanical properties of PLA that are relevant for the finite element model of the pressurization test. These parameters have been stored in the custom library BRIGHT_CAE_Webinar_Materials.sldmat (see Figure 9) provided to the students together with the 3D models shown in Figure 7.
- b) The mould parts are bonded together along their contact surfaces.

Table 2. Physical and mechanical properties of PLA [<https://doi.org/10.1016/j.addr.2016.06.012>]

Mass density ρ [kg/m ³]	Elastic modulus E [MPa]	Poisson's ratio ν [-]	Yield strength Y [MPa]
1252	3500	0.36	59

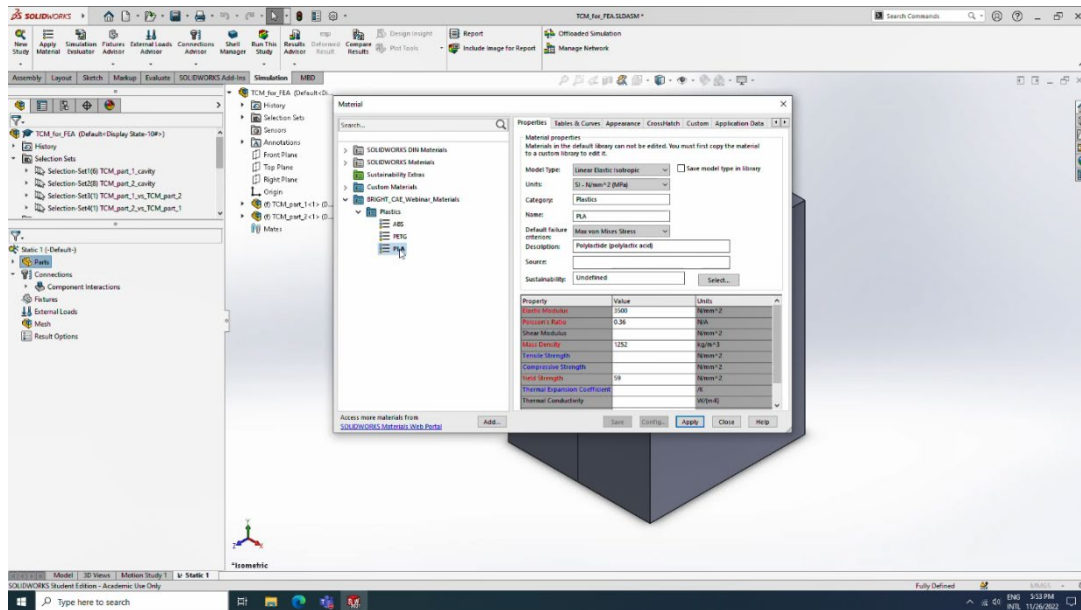


Fig. 9. Associating the PLA material to both mould parts by accessing the BRIGHT_CAE_Webinar_Materials.sldmat library (frame extracted from the recording of the CAE webinar)

The following steps have been performed for preparing the finite element model of the pressurization test:

- Associating the PLA material to both mould parts (Fig. 7) by accessing the BRIGHT_CAE_Webinar_Materials.sldmat library (Fig. 9)
- Specifying the contact interaction between the mould parts: bonded contact (Fig. 10)
- Enforcing a full locking kinematic constraint on the end faces of the mould parts (Fig. 10)
- Defining a unit pressure on the inner surfaces of the mould parts (Fig. 8 and Fig. 10)
Note: The actual values of this load have been specified later as load cases (step (f)).
- Specifying the dimension of finite elements and generating the mesh (Fig. 10)
- Specifying the actual values of the pressure applied to the inner surfaces of the mould parts (Fig. 11): 2 MPa (load case 1), 4 MPa (load case 2), 6 MPa (load case 3), and 8 MPa (load case 4).

This project has been funded with support from the European Commission. This publication [communication] reflects the views only of the authors, and the Commission cannot be held responsible for any use which may be made of the information contained therein.

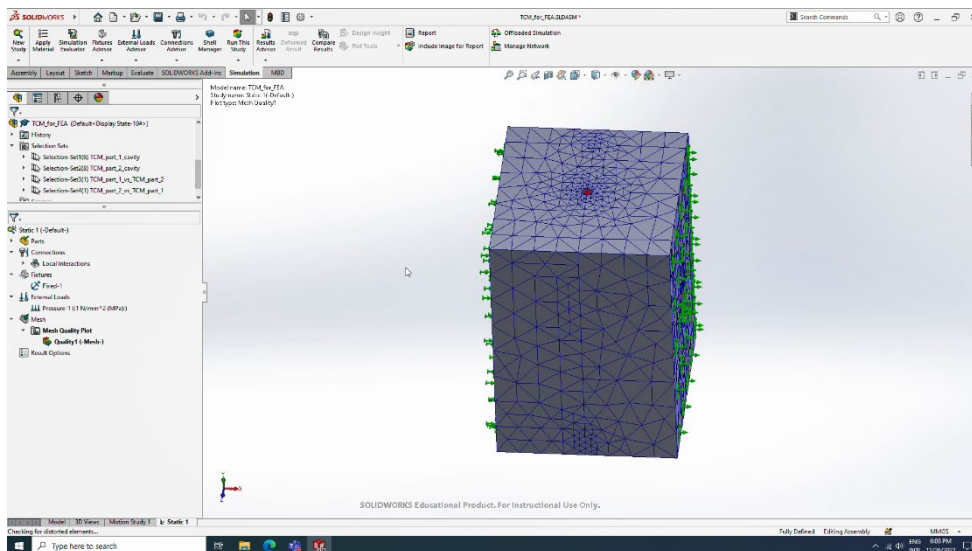


Fig. 10. Finite element model of the pressurization test simulated for evaluating the strength characteristics of the tongue casting mould (frame extracted from the recording of the CAE webinar)

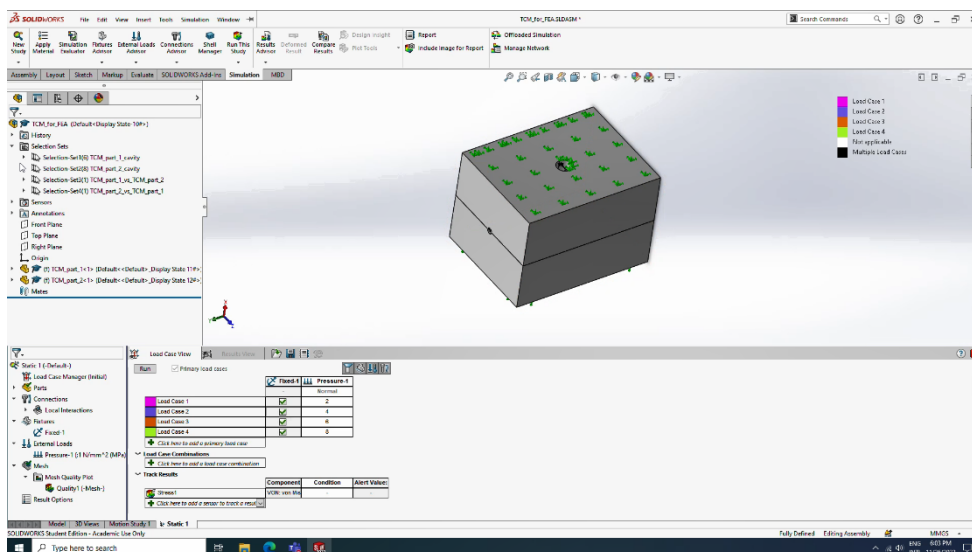


Fig. 11. Specifying the actual values of the pressure applied to the inner surfaces of the mould parts (four load cases): 2 MPa, 4 MPa, 6 MPa, and 8 MPa (frame extracted from the recording of the CAE webinar)

Figures 12 and 13 show the most significant results provided by the finite element analysis module SOLIDWORKS Simulation: distributions of the von Mises equivalent stress in the mould parts for the fourth load case (testing pressure of 8 MPa). Similar distributions associated to other load cases have also been analysed.

This project has been funded with support from the European Commission. This publication [communication] reflects the views only of the authors, and the Commission cannot be held responsible for any use which may be made of the information contained therein.

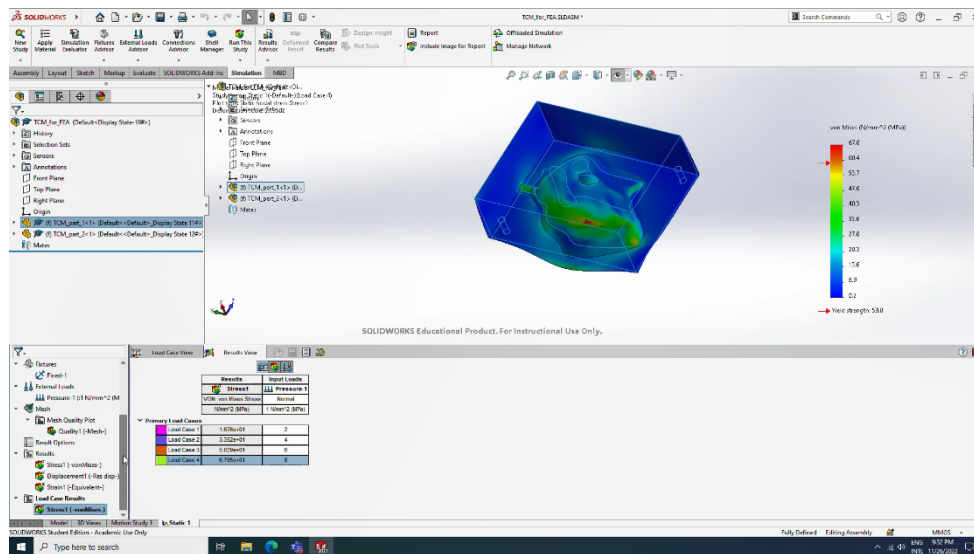


Fig. 12. Colour map showing the distribution of the von Mises equivalent stress in the upper part of the mould for the fifth load case – testing pressure of 8 MPa (frame extracted from the recording of the CAE webinar)

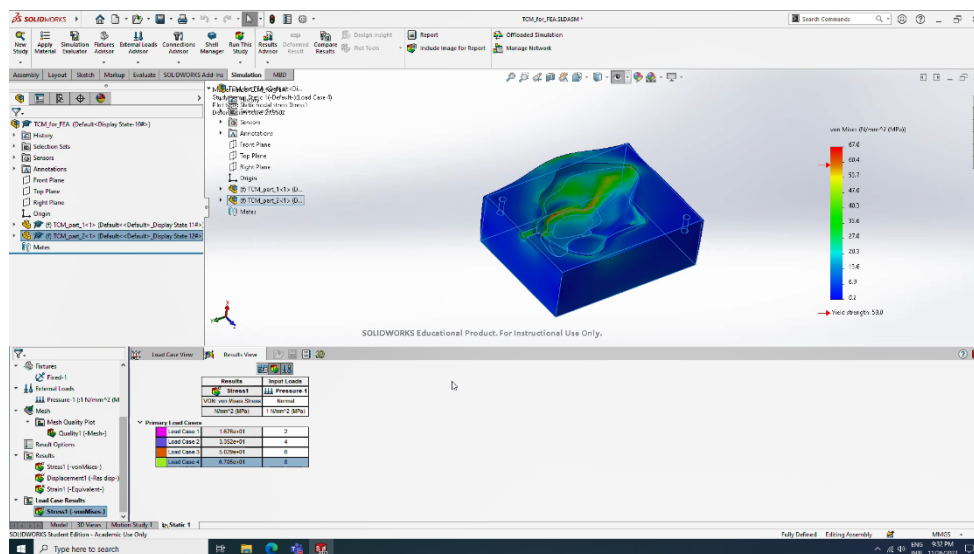


Fig. 13. Colour map showing the distribution of the von Mises equivalent stress in the lower part of the mould for the fifth load case – testing pressure of 8 MPa (frame extracted from the recording of the CAE webinar)

This project has been funded with support from the European Commission. This publication [communication] reflects the views only of the authors, and the Commission cannot be held responsible for any use which may be made of the information contained therein.

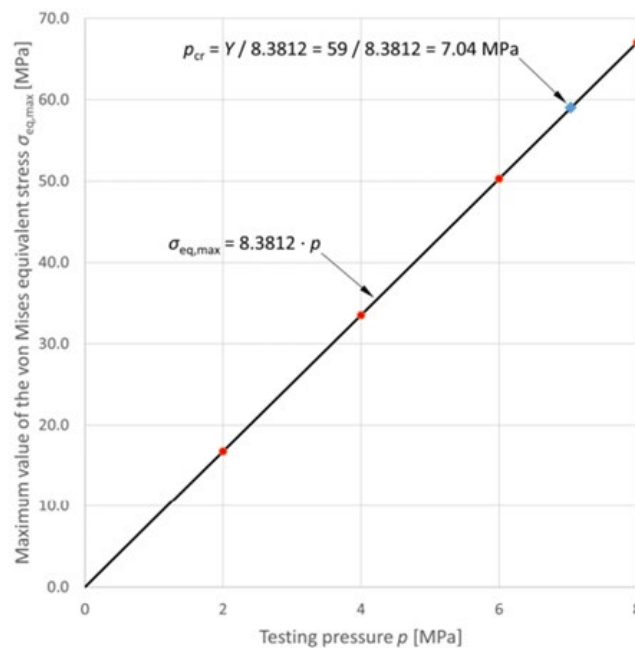


Fig. 14. Maximum values of the von Mises equivalent stress associated to different testing pressures: red dots – numerical results; black path – linear regression; blue diamond – testing pressure at which the maximum value of the equivalent stress equals the yield strength of the PLA material (frame extracted from the recording of the CAE webinar)

The maximum values of the von Mises equivalent stress $\sigma_{eq,max}$ associated to different load cases have been displayed on a diagram showing their dependence on the testing pressure p (Fig. 14). The following conclusions have been formulated after examining the diagram:

- The mechanical response of the mould is well approximated by means of the linear regression $\sigma_{eq,max} = 8.3812 \cdot p$ (see the black path displayed on the diagram).
- This regression can be used to determine the testing pressure at which the maximum value of the equivalent stress equals the yield strength of the PLA material: 7.04 MPa (see the blue diamond displayed on the diagram).
- The finite element analysis shows that the mould exhibits a high strength when loaded by an inner pressure. The critical value of this parameter (7.04 MPa) is much greater than the greatest load that may occur during the casting process.

This project has been funded with support from the European Commission. This publication [communication] reflects the views only of the authors, and the Commission cannot be held responsible for any use which may be made of the information contained therein.

2.2.3. Finite element analysis of a face shield base (3rd case study)

The third case study has focused on evaluating the strength characteristics of a face shield base (Fig. 15) by simulating a dimensional adjustment procedure (Fig. 16). As one may notice in Figure 16, the bilateral symmetry of the shield base allows to perform the finite element analysis on half of its geometric model. Of course, appropriate boundary conditions must be defined on the surfaces generated by the intersection with the symmetry plane. The dimensional adjustment procedure consists in enforcing the rear ends of the shield base to approach the symmetry plane. Only the displacement along the normal to this plane is constrained, its value being gradually increased from 0 (zero) to 7.5 mm.



Fig. 15. Three-dimensional model of the face shield base (frame extracted from the recording of the CAE webinar)

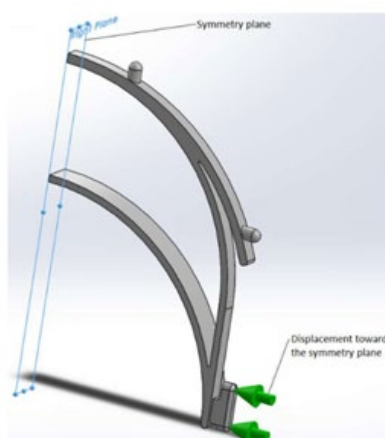


Fig. 16. Dimensional adjustment simulated for evaluating the strength characteristics of the face shield base (frame extracted from the recording of the CAE webinar)

This project has been funded with support from the European Commission. This publication [communication] reflects the views only of the authors, and the Commission cannot be held responsible for any use which may be made of the information contained therein.

The finite element model of the dimensional adjustment procedure has been prepared assuming that the face shield base is made from PETG characterised by an isotropic linear elastic behaviour. Table 3 lists the physical and mechanical properties of PETG that are relevant for the finite element model. These parameters have been stored in the custom library BRIGHT_CAE_Webinar_Materials.sldmat (see Figure 17) provided to the students together with the 3D model shown in Figure 16.

Table 3. Physical and mechanical properties of PETG [<https://doi.org/10.1063/5.0019362>]

Mass density ρ [kg/m ³]	Elastic modulus E [MPa]	Poisson's ratio ν [-]	Yield strength Y [MPa]
1270	1660	0.419	30.3

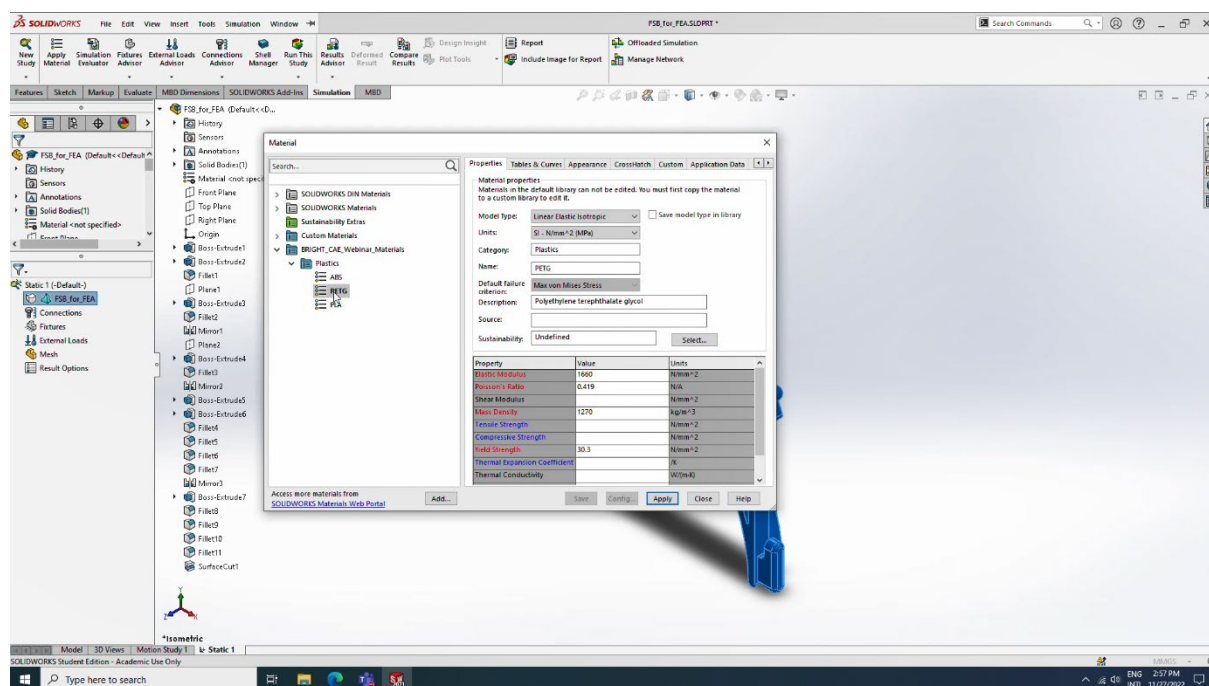


Fig. 17. Associating the PETG material to the face shield base by accessing the BRIGHT_CAE_Webinar_Materials.sldmat library (frame extracted from the recording of the CAE webinar)

The following steps have been performed for preparing the finite element model of the dimensional adjustment procedure:

- a) Associating the PETG material to the face shield base by accessing the BRIGHT_CAE_Webinar_Materials.sldmat library (Fig. 17)

This project has been funded with support from the European Commission. This publication [communication] reflects the views only of the authors, and the Commission cannot be held responsible for any use which may be made of the information contained therein.

- b) Enforcing symmetry-type kinematic constraints on the surfaces generated by the intersection with the symmetry plane of the face shield base (Fig. 16 and Fig. 18)
- c) Enforcing a full locking kinematic constraint on the inner edge of the face shield base generated by the intersection with the symmetry plane (Fig. 16 and Fig. 18)
- d) Enforcing the rear end of the shield base to approach the symmetry plane along a distance of 7.5 mm (Fig. 16 and Fig. 18)

Note: This boundary condition induces significant distortions of the face shield base. Because finite element models affected by significant distortions cannot be analysed for different load cases, the students have been asked to investigate the mechanical response of the face shield base by repeating the simulation of the dimensional adjustment procedure for displacements of the rear end having the following values: 1.5 mm, 3 mm, 4.5 mm, and 6 mm.

- e) Activating the “Large displacement” option of the finite element analysis module SOLIDWORKS Simulation (Fig. 19)

Note: This option must be activated whenever the finite element model is affected by significant distortions.

- f) Controlling the local and global dimensions of finite elements and generating the mesh (Fig. 18).

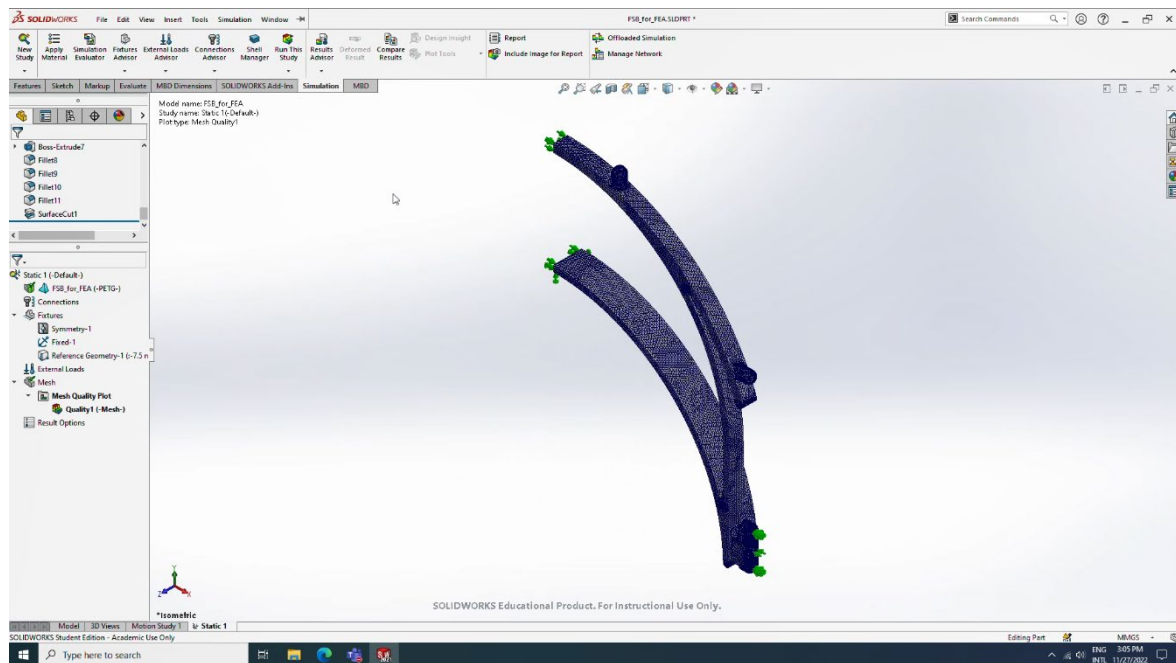


Fig. 18. Finite element model of the dimensional adjustment procedure simulated for evaluating the strength characteristics of the face shield base (frame extracted from the recording of the CAE webinar)

This project has been funded with support from the European Commission. This publication [communication] reflects the views only of the authors, and the Commission cannot be held responsible for any use which may be made of the information contained therein.

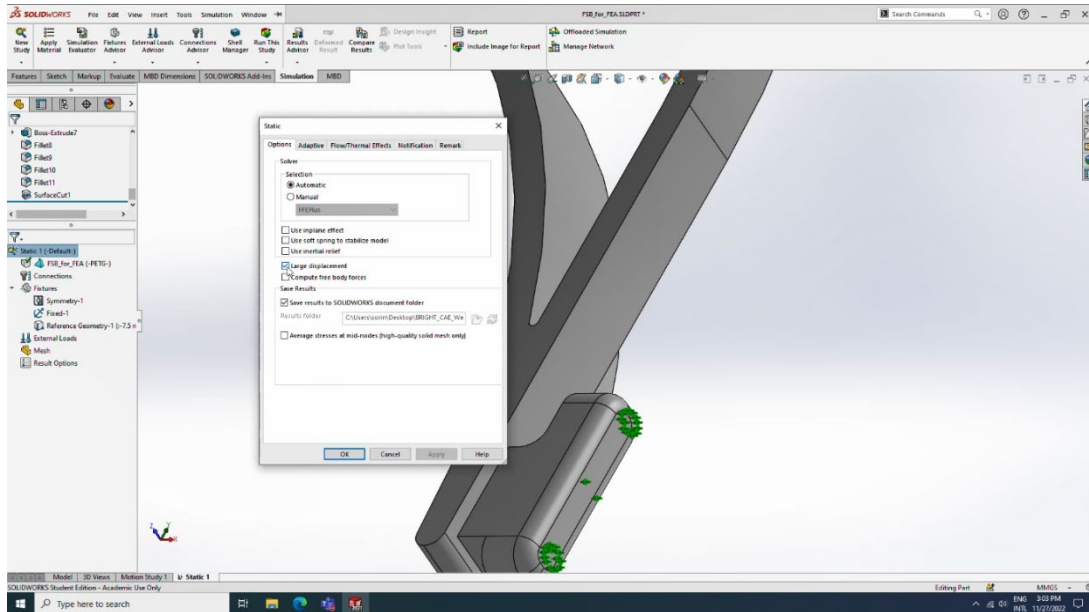


Fig. 19. Activating the “Large displacement” option of the finite element analysis module SOLIDWORKS Simulation (frame extracted from the recording of the CAE webinar)

Figure 20 shows the most significant result provided by the finite element analysis module SOLIDWORKS Simulation: distribution of the von Mises equivalent stress in the face shield base corresponding to the 7.5 mm displacement of its rear end. The maximum values of the von Mises equivalent stress $\sigma_{eq,max}$ corresponding to dimensional adjustments (displacements of the rear end) $d = 1.5$ mm, $d = 3$ mm, $d = 4.5$ mm, $d = 6$ mm, and $d = 7.5$ mm have also been displayed on a diagram (Fig. 21). The following conclusions have been formulated after examining the diagram:

- The mechanical response of the face shield base is well approximated by means of the linear regression $\sigma_{eq,max} = 4.4170 \cdot d$ (see the black path displayed on the diagram).
- This regression can be used to determine the displacement adjustment at which the maximum value of the equivalent stress equals the yield strength of the PETG material: 6.9 mm (see the blue diamond displayed on the diagram).

This project has been funded with support from the European Commission. This publication [communication] reflects the views only of the authors, and the Commission cannot be held responsible for any use which may be made of the information contained therein.

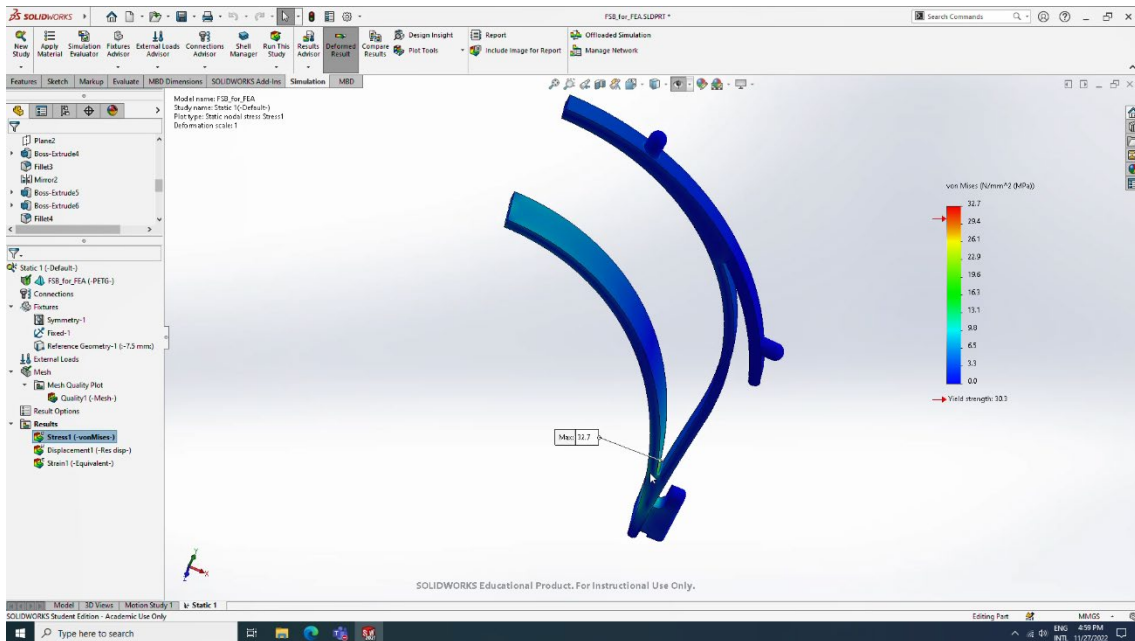


Fig. 20. Colour map showing the distribution of the von Mises equivalent stress in the face shield base corresponding to the 7.5 mm displacement of its rear end (frame extracted from the recording of the CAE webinar)

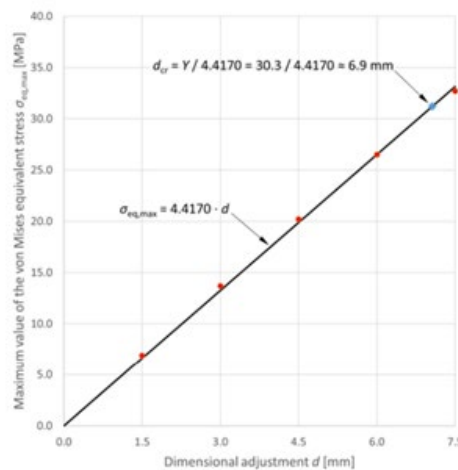


Fig. 21. Maximum values of the von Mises equivalent stress associated to different dimensional adjustments of the face shield base: red dots – numerical results; black path – linear regression; blue diamond – dimensional adjustment at which the maximum value of the equivalent stress equals the yield strength of the PETG material (frame extracted from the recording of the CAE webinar)

This project has been funded with support from the European Commission. This publication [communication] reflects the views only of the authors, and the Commission cannot be held responsible for any use which may be made of the information contained therein.

2.3. Importance of the webinar and of the presented results

The case studies presented in the previous sections of this report demonstrate the capability of finite element analysis programs to assist the designers of medical devices in assessing and improving the quality of their projects, as well as in ensuring the conformity of their projects with the strength requirements by:

- Allowing the designers to investigate the mechanical response of medical devices and to identify the stress concentration areas (see Figures 5, 12, 13, and 20)
- Allowing the designers to evaluate the load-carrying capacity of medical devices i.e., the level of the external loads for which the maximum stress equals an upper limit (see Figures 6, 14 and 21).

If properly used, finite element analysis programs increase the efficiency of the design process and speed up the development of new products. These advantages are essential in pandemic times.

3. Conclusions

By attending the CAE webinar, students have acquired a basic knowledge of applying the finite element method in the design of medical devices. This knowledge is useful to any specialist involved in the development of such products. It also improves the quality of his/her collaboration with medical institutions or manufacturers of medical devices. The case studies presented in this webinar can equally be used as self-training resources or teaching materials for MSc study programs.

This project has been funded with support from the European Commission. This publication [communication] reflects the views only of the authors, and the Commission cannot be held responsible for any use which may be made of the information contained therein.